Current Research in Food Science 5 (2022) 1740–1749

Contents lists available at ScienceDirect

Current Research in Food Science

journal homepage: www.sciencedirect.com/journal/current-research-in-food-science

Quantitative proteomic analysis provides insight into the survival mechanism of *Salmonella* typhimurium under high-intensity ultrasound treatment

Wei Luo [a,1], Jinqiu Wang [a,1], Yan Chen [a], Yixu Wang [a], Rui Li [b], Jie Tang [a], Fang Geng [a,*]

[a] Institute for Egg Science and Technology, School of Food and Biological Engineering, Chengdu University, No. 2025 Chengluo Avenue, Chengdu, 610106, China
[b] Engineering Research Center of Sichuan-Tibet Traditional Medicinal Plants, Chengdu University, No. 2025 Chengluo Avenue, Chengdu, 610106, China

ARTICLE INFO

Keywords:
Ultrasound
Salmonella
Proteome
Energy metabolism
Two-component system
ABC transporter

ABSTRACT

The survival mechanism of *Salmonella* treated with high-intensity ultrasound (HIU) should be explored to further enhance the bactericidal efficacy of HIU. In this study, culturable *Salmonella* was reduced by applying HIU. Electron microscope imaging revealed that HIU caused the disintegration of cell structure and leakage of intracellular substances. For the *Salmonella* after the HIU treatment, key enzymes of the tricarboxylic acid [TCA] cycle were significantly downregulated, which led to a reduced ATP content (45.25%–75.00%), although ATPase activity was augmented by 33.82%–60.64% in the *Salmonella*. Accordingly, surviving *Salmonella* could have tolerated the stress of HIU by upregulating their environmental sensing (two-component system), chemotaxis (bacterial chemotaxis), substance uptake (ABC transporter), and ATP production (oxidative phosphorylation). Therefore, synergistically blocking the ATP production, signal transduction, or substance intake of *Salmonella* offer promising potential strategies to improve the bactericidal effect of HIU in industrial food processing.

1. Introduction

Salmonella is a foodborne pathogenic microorganism commonly found in dairy, meat, poultry, egg products, fresh fruit/vegetable products, and even in some low-moisture foods (Kaavya et al., 2021). Foodborne illnesses caused by *Salmonella* pose a worldwide threat to food safety and are of mounting public concern. According to data reported by China's National Foodborne Illness Outbreak Surveillance System from 2003 to 2017, a total of 899 outbreak reports were associated with *Salmonella*, resulting in 11 351 hospitalizations and 4 deaths (Li et al., 2020). According to the European Food Safety Authority's 2020 report, the second most commonly reported foodborne gastrointestinal infection in humans in EU MS and non-MS countries is caused by *Salmonella* (a total of 52 702 cases reported) (European Food Safety et al., 2021). To effectively control *Salmonella*, various chemical disinfectants such as chlorine, iodine, and hydrogen peroxide are often used to treat foods and utensils in food processing yet are prone to forming chemical residues (Cacciatore et al., 2020). Furthermore, adding chemical preservatives (such as potassium sorbate) to food products has raised concerns about their health risks (Pereira Batista et al., 2019). Heat treatment can effectively kill or inhibit *Salmonella*, but this usually entails a reduction in the nutritional value and consumer preference of the heat-sensitive foods, such as liquid egg products and juice drinks (Bi et al., 2020; Hu et al., 2016). Consumer demand for the safety, nutritional value, and sensory enjoyment of food has increased, making the traditional sterilization technology more challenging to implement (Chen et al., 2020). Accordingly, this has spurred further research and exploration of new bacteriostatic and bactericidal techniques that are safer, more efficient, and also energy saving.

Ultrasound, a physical processing technology widely used in food processing, can effectively achieve bacterial inhibition by producing an acoustic cavitation effect and it is very environmentally friendly (Seo et al., 2019). Research findings have proven the lethal effect of ultrasonic treatments on *Salmonella*. For example, Bi et al. (2020) showed that sonication at 968 W/cm^2 and 35°C for 20 min effectively reduced *S.* typhimurium by about 3.31 log in liquid eggs. Liu et al. (2021a) also found that sonication at 200 W and 26 kHz for 5 min killed 1.4 log CFU/g of pathogenic bacteria, such as the *Salmonella* on the surface of sprouts. Moreover, the combined use of an ultrasonic treatment and chemical antibacterial agents usually has a synergistic effect (He et al.,

* Corresponding author.
E-mail address: gengfang@cdu.edu.cn (F. Geng).
[1] These authors contributed equally to this work.

https://doi.org/10.1016/j.crfs.2022.09.029
Received 28 May 2022; Received in revised form 21 August 2022; Accepted 30 September 2022
Available online 9 October 2022

2021). For instance, ultrasound increases the bactericidal effect of sodium dichloroisocyanurate, resulting in a 4-log reduction of *Salmonella* adhering to cabbage (Duarte et al., 2018). The number of *S. enterica* in cherry tomatoes can be reduced to safe levels by a combined treatment consisting of ultrasound and lactic acid (José et al., 2021).

Zhang et al. (2021) reported that ultrasound and phenyllactic acid exert synergistic antimicrobial effects by significantly disrupting the cell membrane structure of bacterial cells in *Salmonella* biofilms, thereby leading to the leakage of internal components and inactivation of internal enzymes. Yet the combined use of ultrasound and certain chemical inhibitors, such as peracetic acid or phosphoric acid, need not always generate a synergistic effect (Laranja et al., 2021). Evidently, much research is concerned with evaluating the antimicrobial effects of ultrasound (alone or in a combined application) on *Salmonella* in the relevant food matrix. However, an ultrasound treatment is usually unable to kill all *Salmonella* present to ensure food safety, even when applying high-ultrasound power or it in combination with antibacterial agents. Therefore, the mechanisms by which *Salmonella* cells survive under ultrasound treatment needs to be explored, whose findings could point to effective methods to enhance its bactericidal effect against this genus of food pathogens. In recent studies, proteomics has become a useful tool to study the bacterial response to stress in food processing and storage-related stresses. For example, Qi et al. used proteomics to study the antibacterial effect of sublethal concentrations of thymol on *Salmonella enterica* serovar Typhimurium (Qi et al., 2020). However, current proteomic studies on ultrasonically treated *Salmonella* have not been identified.

Here, the bacteriostatic effects of high-intensity ultrasound (HIU) treatments on *Salmonella* typhimurium were evaluated through plate counting and observations of bacterial cell structure. And the HIU-treated *Salmonella* cells were subjected to label-free quantitative proteomic analysis with the untreated *Salmonella* as the control. Differentially expressed proteins (DEPs) in these HIU-treated *Salmonella* were screened; then, the physiological processes enabling *Salmonella* to resist the stress induced by HIU were investigated and this bacteria's corresponding underlying survival mechanism discussed. It was anticipated this study would provide insights into the survival mechanism of HIU-treated *Salmonella* typhimurium and help to lay a foundation for further enhancing the bactericidal effects of HIU.

2. Materials and methods

2.1. Bacterial strains and incubation conditions

The *Salmonella* typhimurium CGMCC1.1859 (original number: ATCC14028) was purchased from the China General Microbiological Culture Collection Center (CGMCC, Beijing, China). The *Salmonella* strain was first activated at 37°C in an incubator (150 rpm; ZWY-1102C, Shanghai Zhicheng Instrument Manufacturing Co., Ltd., Shanghai, China) with nutrient broth medium (NB: 10.0 g peptone, 3.0 g beef extract, 5.0 g NaCl, make up to 1 L with sterile water; Haibo Biotechnology Co., Ltd., Qingdao, China) for 12 h. The activated bacteria were then separated on nutrient agar (NA: 10.0 g peptone, 3.0 g beef extract, 5.0 g NaCl, 15.0 g agar, make up to 1 L with sterile water; Haibo Biotechnology Co., Ltd., Qingdao, China) and incubated at 37°C for 24 h. Individual colonies were collected from this nutrient agar, then transferred to conical flasks containing 20 mL of nutrient broth, and incubated at 150 rpm for 11 h at 37°C. To obtain their initial stable growth (stationary phase), 0.2 mL of culture solution was transferred to 20 mL of fresh nutrient broth medium and the incubation continued for 11 h with shaking. Next, 2 mL was aspirated from the initial stable bacterial solution and centrifuged (at 1685×*g* for 5 min), then resuspended with phosphate buffered saline (PBS, pH 7.2). The final concentration was set to 1.50×10^7–4.00×10^7 CFU/mL by adding 1 mL of the diluted resuspension solution to 25 mL of PBS, and the exact working concentration used in HIU treatment was determined by plate counting.

2.2. HIU treatments

In this experiment, a probe sonicator (SCIENTZ-IID, Ningbo Xinzhi Biotechnology Co., Ltd., Ningbo, China) was used to inhibit bacteria under different durations and power setting conditions. Its probe was 6 mm in diameter and 10 mm in depth; the pulse interval was turned on for 3 s and then off for 3 s. HIU treatments were carried out with a water bath maintained at below 20°C (Xie et al., 2020). Untreated *Salmonella* served as the negative control. The power density of HIU (D, in units of W/mL) was calculated this way: D = P/V, where P is the HIU power and V is the volume of the medium (26 mL) (Li et al., 2017).

2.3. Enumeration of viable Salmonella cells

The untreated and HIU-treated samples under different sonication conditions (at 90 W, 180 W, 270 W, and 360 W; each lasting 5 min, 15 min, or 25 min, for 12 treatment combinations) were taken and serially (1:10) diluted using an 0.85% (w/v) NaCl solution, from which a certain volume (0.1 mL) was applied to plate count agar (PCA) in duplicate, then this incubated at 37°C for 24 h. The inactivation effect was determined based on the log(N) of this colony count, where N (CFU/mL) is the number of residual colonies after the HIU treatment. The HIU treatments of 270 W for 15 min (US-270), 90 W for 25 min (US-90), and 360 W for 5 min (US-360) were selected for further analysis.

2.4. Evaluation of Salmonella cell disintegration

2.4.1. Scanning electron microscopy (SEM)

The suspensions of *Salmonella* with or without HIU treatments were centrifuged (at 6790×*g* for 10 min at 4°C), and the collected *Salmonella* cells were washed thrice with PBS. Then the *Salmonella* cells were fixed by a glutaraldehyde solution (2.5%, at 4°C for 12 h), and later dehydrated by a gradient series of ethanol solutions (30%–100%; 20 min for each concentration). After this gradient dehydration, 10-μL drops were aspirated onto slides and allowed to air-dry naturally, then surface-sprayed with gold, after which surface changes in their bacteria were observed via SEM (Thermo Scientific Apreo 2C, Thermo Fisher Scientific Co., China) (Geng et al., 2021a). Three biological replicates of each group of samples were used, from which typical images are presented.

2.4.2. Transmission electron microscopy (TEM)

Untreated and HIU-treated (US-270, US-90, US-360) *Salmonella* were collected by centrifugation and rinsed three times in PBS (pH 7.2) buffer, then fixed successively by a 2.5% glutaraldehyde solution for 12 h and a 1% osmium acid solution for 2 h (rinsed thrice with PBS after each treatment). Dehydration was carried out using a gradient series of ethanol solutions (30%–95%; 15 min for each concentration), followed by treatment with 100% ethanol for 20 min and acetone for 20 min (Geng et al., 2021b). The dehydrated samples were first embedded and then sectioned by a frozen ultrathin sectioning machine (Leica EM UC7, Leica Microsystems, Germany) to yield sections 70–90 nm in width. These sections were stained with a lead citrate solution and a 50% ethanol saturated uranyl acetate solution (5–10 min for each staining). After drying, the sections were imaged by TEM (Hitachi-7800, Hitachi Scientific Instruments, Ltd., Japan). Each group of samples was repeatedly prepared and imaged three times, from which typical images are presented.

2.4.3. Changes in extracellular conductivity

The untreated and three HIU-treated (US-270, US-90, US-360) bacterial suspensions were taken and centrifuged at 6790×*g* for 15 min at 4°C. The ensuing supernatant was removed to determine the conductivity of the solutions, as measured by a conductivity meter (DDS-11C type, Shanghai Yidian Scientific Instruments Co., Ltd., China). This determination was repeated three times for each sample.

2.4.4. Determination of intracellular protein leakage

The HIU treatment (US-270, US-90, US-360)-induced intracellular protein leakage of *Salmonella* was evaluated. An ultrafiltration tube (3000 Da molecular weight cut-off; Merck KGaA, Darmstadt, Germany) was used to concentrate (100-fold) the leaky intracellular proteins in the supernatant of the bacterial suspension. Protein contents of the supernatant concentrations were measured, using the Bradford Protein Assay Kit (Shanghai Biyuntian Biotechnology Co., Ltd., Shanghai, China), with each sample having five replicates. Furthermore, the supernatant concentrations were subjected to SDS-PAGE electrophoresis; typical images from three replicates were selected for the presentation of these results (Wang et al., 2021).

2.5. Label-free quantitative proteomic analysis of Salmonella after HIU treatment

2.5.1. Protein extraction and digestion

Untreated and HIU-treated (US-270, US-90, US-360) bacterial cells were centrifuged at 6790×*g* for 10 min at 4°C, rinsed in PBS (pH 7.2) buffer three times, and then stored at −80°C (cryopreservation) (Li, et al., 2020; Luo et al., 2021). The collected *Salmonella* cells were lysed by the lysis solution (pH 8.1, 100 mM Tris-HCl, 1.5% SDS) and the total protein was precipitated through acetone. The protein precipitate was incubated for 1 h at 37°C with the addition of a complex solution (8 M Urea, 100 mM Tris-HCl) and dithiothreitol (DTT). Protein extract was treated with iodoacetamide (IAA, 40 mM). Finally, each sample was diluted to a urea concentration below 2 M by adding to it a Tris-HCl buffer (100 mM) (Wang et al., 2022a). The same amount of protein (determined by the Bradford method) was taken for the following digestion processing and proteomic analysis (Geng et al., 2018). Trypsin was mixed with protein (at a ratio of 1:50) and shaken for 12 h at 37°C for the latter's digestion. To terminate this digestion process, trifluoroacetate (TFA) was added, after which the supernatant of the digestion was desalted in a Sep-PakC_{18} column. After drying, all peptide samples were stored at −20°C.

2.5.2. LC–MS/MS

Mass spectrometry data was acquired using a LC–MS/MS system (OrbitrapExploris 480 mass spectrometer in tandem with of EASY-n LC 1200 liquid phase). The peptide samples were first separated by a C18 analytical column (1.9 μm, 75 μm × 25 cm, 100 Å). The elution gradients were established using mobile phase A (0.1% formic acid) and mobile phase B (0.1% formic acid, 80% CAN): this began with going from 6% to 25% mobile phase B over 68 min, followed by an increase to 45% B over 14.5 min, an increase to 80% B over 0.5 min, and then held at 80% B for 7 min, at a flow rate of 300 nL/min (Liu et al., 2020). The separated peptides were ionized by a nano-electrospray ion source (2.3 kV). Here, the Data Dependent Acquisition mode was applied to acquire the mass spectrometry data, with each scan cycle containing a full MS scan (resolution, 60 K; automatic gain control, 300%; maximum injection time, 20 ms; scan range, 350–1500 *m/z*), and 20 subsequent MS/MS scans (resolution, 15 K; automatic gain control, 100%; maximum injection time, auto; cycle time, 2 s) (Wang et al., 2022b).

2.5.3. Data processing

For the mass spectrometry data retrieval, the Andromeda algorithm was used in MaxQuant (v1.6.6) software, and the database used for the search was UniProtKB (*Salmonella enterica*; date: 20211104). The main search parameters and screening criteria were as follows: carbamidomethyl (C) for fixed modifications, oxidation (M) for variable modifications, trypsin/P for enzymatic digestion. Finally, the protein and peptide search results were screened with a 1% false discovery rate (Liu et al., 2021b).

Subcellular localization of the identified proteins was first annotated using MultiLoc2 (https://abi-services.informatik.uni-tuebingen.de/multiloc2/webloc.cgi). Then the proteins' GO and KEGG annotations were carried out using the BLAST comparison tool (BLASTp, e-value ≤ $1e^{-5}$) (Ashburner et al., 2000; Ross and P, 2004). Principal component analysis (PCA) and Pearson's correlation coefficient (r) analysis were conducted to assess the intra-group reproducibility and the difference between groups.

2.6. ATP content and ATPase activity of Salmonella

The intracellular ATP contents of the untreated and three HIU (US-270, US-90, US-360) *Salmonella* samples were measured using an enhanced ATP assay kit (S0027, Biyuntian Biotechnology Co., Ltd., Shanghai, China), this based on fluorophore enzymes (firefly) catalyzing the production of fluorescence by fluorophore requiring energy from ATP. First, the method was the same as described above for the SEM assay, and the untreated and HIU (US-270, US-90, US-360) treated *Salmonella* cells were collected. The *Salmonella* cells were lysed using the lysis buffer according to the method in the kit, and the supernatant was taken after centrifugation. The ATP assay working buffer was taken into the 96-well plate, stood for 3–5 min, then sample lysate supernatant was add and chemiluminescence was detected. Here, a multifunctional microplate reader (Synergy HTX, BioTek Instruments, Inc., Winooski, VT, USA) was used for the determination of chemiluminescence values, and this assay repeated three times per sample.

The changes in intracellular ATPase activity of *Salmonella* untreated and treated with HIU (US-270, US-90, US-360) were detected using the Ultra Trace Total ATPase Test Kit (A070-1, Jiancheng Institute of Biological Engineering, Nanjing, China). This kit is based on the principle that ATPase can decompose ATP to produce ADP and inorganic phosphorus; hence, the amount of inorganic phosphorus can be measured to determine the level of ATPase activity. Here ATP enzyme activity was calculated according to the kit's formula, after detecting the OD_{636} value using a multifunctional enzyme standard (Synergy HTX, BioTek Instruments, Inc.). This assay was repeated three times.

2.7. Statistical analysis

The data are expressed as the mean and standard deviation (SD). Statistical analyses performed included one-way analysis of variance (ANOVA) using GraphPad Prism 8.0 software, for which differences were considered significant at $P < 0.05$.

3. Results and discussion

3.1. Inhibitory effect of HIU treatment on Salmonella

In response to the HIU treatment, the number of viable cells of *Salmonella* all decreased, and this reduction became more pronounced with prolonged exposure time to HIU (Fig. 1A). Further, the inhibition effect was enhanced with more HIU power applied. The number of viable *Salmonellae* decreased by about 2.87 log after 360 W and 25 min of HIU, indicative of a good bacteria removal effect. To evaluate the inhibitory effect of the intensity and duration of HIU on *Salmonella* and its related mechanisms, US-270 (high intensity-medium time; D = 10.38 W/mL, 0.98-log reduction), US-90 (low intensity-long time; D = 3.46 W/mL, 0.61-log reduction), and US-360 (high intensity-short time; D = 13.85 W/mL, 0.60-log reduction) were selected for the analyses that follow. Similar inhibition results were reported in previous studies, such as the 3.31-log reduction of *S.* typhimurium in liquid eggs after its treatment at 968 W/cm^2 and 35°C for 20 min, and the decrease of ca. 2 log of *Salmonella* in sprouts exposed to 200 W and 26 kHz for 5 min (Bi et al., 2020; Liu et al., 2021a). What should be kept in mind is that we used a PBS solution, which differs from the actual food matrix, and it may have attenuated the ultrasound effect. Although HIU treatments can substantially inhibit *Salmonella*, the bactericidal effect cannot ensure food safety, which limits the practical application of HIU.

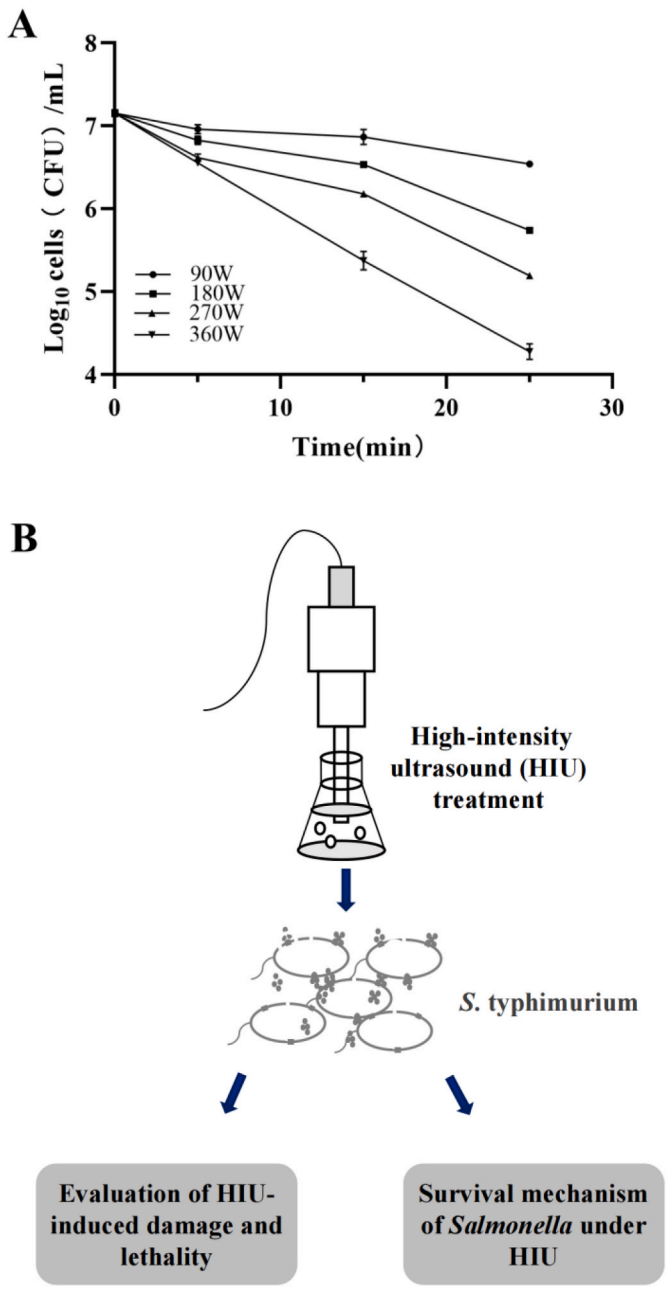

Fig. 1. Effect of high-intensity ultrasound (HIU) treatment upon *Salmonella*. (A) Changes in the number of cultivable *Salmonella* after HIU treatment applications; **(B)** the framework to study the lethality of *Salmonella* induced by HIU and the survival mechanism of *Salmonella* after the HIU treatment.

3.2. Disintegration and lethality of Salmonella induced by HIU

Why can a small amount of *Salmonella* survive after HIU treatment? It is a paramount question that merits study. To address it, here the disintegration and lethality of *Salmonella* induced by HIU were first evaluated and discussed; then we focused on the changes in physiological processes within *Salmonella* cells after undergoing HIU, using a quantitative proteomic analysis to explore the survival mechanism of *Salmonella* treated with HIU (Fig. 1B).

3.2.1. Structural damage

The destruction of bacterial cell walls/membranes caused by ultrasound is often considered the main mechanism underpinning ultrasound-induced bacterial cell damage (Dai et al., 2020). In our study, we used SEM and TEM to observe the *Salmonella*'s morphological surface damage and internal structural changes in response to HIU. The SEM results showed that most of the untreated *Salmonella* cells (CK) were rod-shaped, with an intact surface morphology, and the bacterium featured a flat and smooth surface (Fig. 2A and a). In stark contrast, the HIU treatment resulted in surface depression, deformation, boundary fusion, disintegration, and leakage of intracellular substances of *Salmonella* (Fig. 2B–D and 2b–d). After exposure to the US-270 treatment, a considerable part of the *Salmonella* cells disintegrated and an abundance of intracellular substances were leaked. Compared with that, treatment with US-90 or US-360 mainly resulted in surface depression and deformation, with minor disintegration and less leakage of intracellular substances.

The structural damage of *Salmonella* cells after their HIU treatment was further evaluated by TEM. The microscopic imaging revealed untreated *Salmonella* cells having a clear wall-membrane structure and an electron transparent zone in their cytoplasm. Evidently some clusters (tens of nanometers) were distributed in the cytoplasm of *Salmonella*, which may be non-membrane-bound functional cellular condensates formed by biomacromolecule interactions (Fig. 2E and e). After the HIU treatment, the most obvious changes were the reduction of the electron transparent zone in the cytoplasm, the disappearance of non-membrane-bound organelles in the cytoplasm, and the damaged cell wall/membrane structures (Fig. 2F–H and 2f–h). Additionally, some membraneless cells and empty cells were observed, indicating the occurrence of cell membrane damage and substantial leakage of cytoplasmic contents. These electron microscopy results strongly suggest that treating *Salmonella* with HIU severely affects the external structural integrity of its cells and also has destructive impacts on its internal non-membrane-bound functional cellular condensates.

3.2.2. Intracellular substances leakage

Based on the above SEM and TEM results, showing that an HIU treatment severely disrupts the *Salmonella* cell structure, the leakage of intracellular substances (proteins and ions) induced by HIU was further explored. After exposure to HIU, the conductivity of the supernatant of *Salmonella* suspensions increased by 13.47%–18.10% over the control (untreated group) (Fig. 2I). The most significant increase in conductivity values was observed under the US-360 treatment. Greater conductivity is to some extent an indication of altered bacterial membrane permeability and an abnormal outflow of some ionic components (Li et al., 2018; Tao et al., 2011). For instance, Li et al. found that trace amounts of K^+ flowed out through ion channels of *E. coli* cells after treating them with HIU and thus significantly increased the extracellular K^+ concentration (Li et al., 2018). Besides ions, some macromolecular electrolytes (such as proteins) would have leaked into the supernatant of the bacterial suspension due to the disintegration and destruction of *Salmonella*'s cell wall membrane, this also promoting conductivity.

Total protein content in the supernatant of the *Salmonella*'s suspension was 10.37, 9.47, and 7.56 μg/mL after the US-270, US-90, and US-360 treatments, respectively, corresponding to a 27.62–38.30-fold increase over the untreated group (Fig. 2J). The results also uncovered differential extracellular protein content at similar lethality (between US-90 and US-360), perhaps due to the influence of the ultrasound duration. From the follow-up SDS-PAGE analysis of protein composition in the supernatant of the *Salmonella* suspension, we learned that the number of protein bands and their position on electrophoresis gel (molecular weight) was similar among the three HIU treatments (Fig. 2K). However, the gray values of their protein bands differed, which was consistent with the determination of protein content.

The above findings suggest the HIU treatment caused *Salmonella*'s disintegration and leakage of intracellular substances, with the degree of damage correlated with the intensity and duration of ultrasound. Among them, the high ultrasound intensity increases the permeability of bacterial membranes within a short period, prolonged treatment with low intensity ultrasound allows further accumulation of cell structural

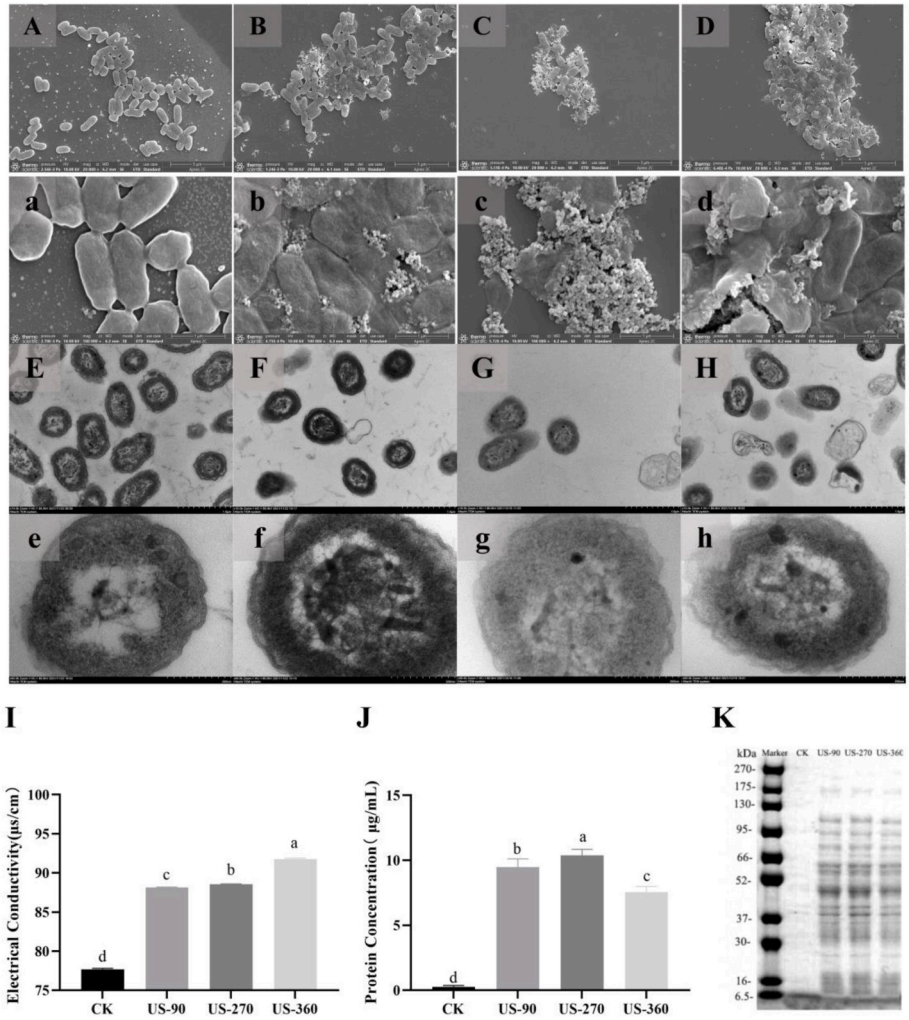

Fig. 2. Changes in the structure of *Salmonella* after their high-intensity ultrasound (HIU) treatment. (A–D) SEM images of untreated (A, a), US-90 treated (B, b), US-270 treated (C, c), and US-360 treated (D, d) *Salmonella*. **(E–H)** TEM images of untreated (E, e), US-90 treated (F, f), US-270 treated (G, g), and US-360 treated (H, h) *Salmonella*. **(I)** The conductivity, **(J)** protein content, and **(K)** SDS-PAGE of the supernatant of the *Salmonella* suspension. CK, untreated group; US-90, 90 W for 25 min; US-270, 270 W for 15 min; US-360, 360 W for 5 min.

damage, while the combination of high intensity and long duration is necessary for bacterial disintegration and death. Therefore, structural damage caused by HIU not only directly leads to the breakdown and death of *Salmonella* cells but it could also enhance the bactericidal effect if combined with chemical antibacterial agents.

3.3. Quantitative proteomic analysis of Salmonella after HIU treatment

3.3.1. Comparison of protein profiles

A total of 2920 proteins were identified from all four groups of *Salmonella* samples (CK [control], and US-90, US-270, US-360 treatments). Their PCA revealed differences between the groups (Fig. 3A). The PCA plot of the four groups showed a separation along the PC1 dimension. The separation was greater in the US-270 group compared with the other three groups. Similar results were obtained for the analysis of correlations between groups (Fig. S1). Altogether, these multivariate statistical analysis results suggested that the *Salmonella* protein profiles were changed by the HIU treatments.

A total of 1017 differentially expressed proteins (DEPs) were screened according the criteria of FC (Fold Change) > 1.5 (or FC < 0.67) and $P < 0.05$ (Table S1). The largest number of DEPs (988 DEPs) was found in the US-270 vs. CK comparison, whereas only 10 DEPs were found for US-90 vs. US-360 (Fig. 3B). A total of 144 DEPs overlapped in the comparisons between the three HIU treatment groups and the CK group (Fig. S2A). This suggested those DEPs are common response proteins of *Salmonella* to HIU exposure levels. The functional classification of these DEPs shows that these proteins are mainly involved in "catalytic activity", "binding", "transport activity", "cellular process", and "metabolic process" (Fig. S2B). These GO classification results also indicate, to some extent, that different conditions of the HIU treatment could affect some proteins on the cell membrane that have transport catalytic as well as binding activities.

3.3.2. Subcellular distribution of DEPs

Of the 2920 *Salmonella* proteins identified, 2409 were annotated; 64.96% of them were annotated as "cytoplasmic" and 26.40% as "cytoplasmic membrane". By contrast, most of the DEPs in *Salmonella* induced by HIU treatment were localized to the "cytoplasmic membrane", these accounting for 52.78%–76.30% of the total DEPs found (Fig. 3C). The subcellular localization distribution of DEPs induced by US-90 and US-360 behaved similarly, suggesting that degree of change was correlated with their lethal effects. Notably, among the 62 annotated *Salmonella* "extracellular membrane" proteins, 44, 10, and 22 of them were differentially expressed in response to the US-270, US-90, and US-360 treatments, respectively. These results indicated the "cytoplasmic membrane" and "extracellular membrane" of *Salmonella* are the cellular components most affected by HIU.

Among the 117 periplasmic proteins annotated, treatment with US-270 caused changes to the expression of 48 of them (14 upregulated, 34 downregulated), whereas US-90 and US-360 caused the upregulation of only 4 and 6 of them, respectively. These periplasmic proteins can specifically bind nutrients, such as amino acids, sugars, and other compounds (Davies et al., 2021; Suginta et al., 2018). These results lend compelling support to the idea that bacteria can respond to osmotic

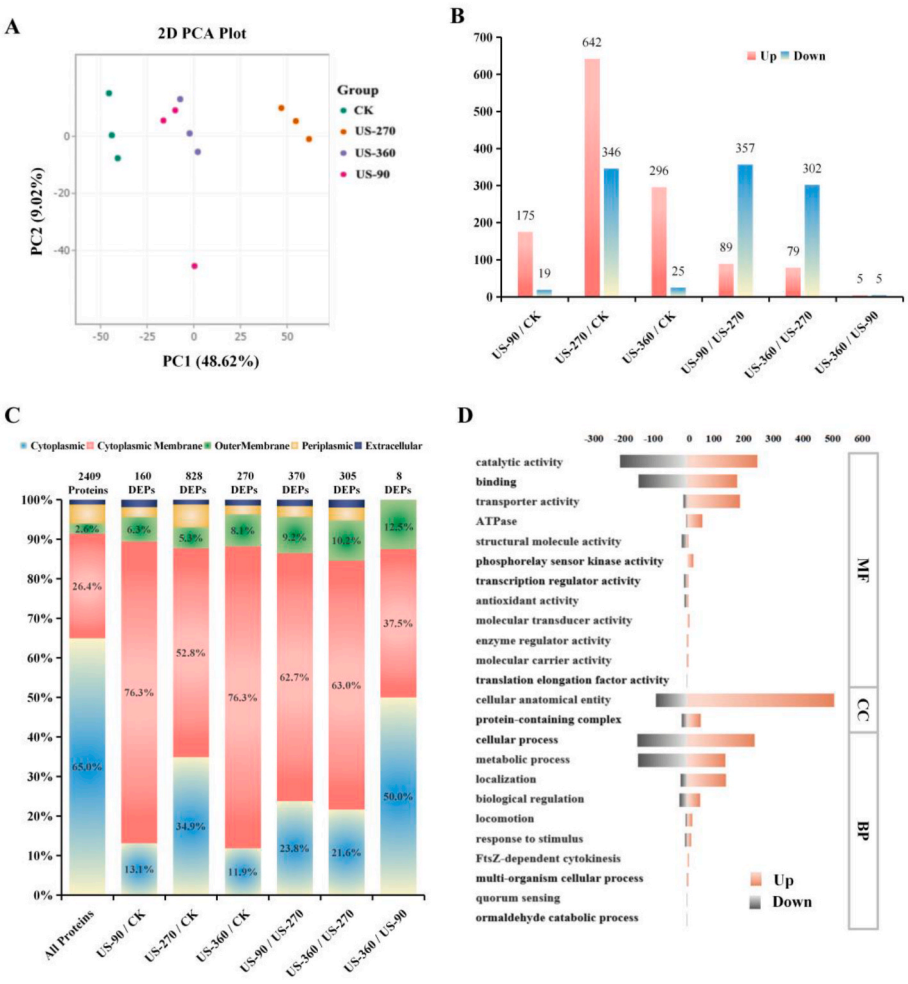

Fig. 3. Quantitative proteomic analysis of *Salmonella* after their high-intensity ultrasound (HIU) treatment. (A) Principal component analysis of the protein profiles of *Salmonella* after their HIU treatment. **(B)** The number of differentially expressed proteins (DEPs) in the pairwise comparison between groups. **(C)** Subcellular distribution of DEPs after the HIU treatment. **(D)** GO analysis of DEPs after the HIU treatment. CK, untreated group; US-90, 90 W for 25 min; US-270, 270 W for 15 min; US-360, 360 W for 5 min.

stress by releasing periplasmic proteins outside their cells. These results also fully corroborate those observed here by SEM and TEM.

3.3.3. GO and KEGG analysis of DEPs

The functions of the 1017 DEPs of *Salmonella* induced by the HIU treatment were classified by their GO analysis. Within the "biological processes" category, the HIU-treated DEPs were distributed among 10 main terms, of which "cellular processes", "metabolic processes", and "localization" are the most prominent (Fig. 3D). The "localization" and "metabolic processes" terms deserve special attention, with the number of DEPs associated with "localization" upregulated surpassing those downregulated, and vice versa for "metabolic processes". Within the "molecular function" category, "catalytic activity", and "binding" were the predominant terms.

To further clarify the potential regulatory pathways of HIU-treated *Salmonella*, KEGG annotation and enrichment analysis of the DEPs were carried out. The DEPs of US-90-treated *Salmonella* were annotated to 54 pathways, of which 5 pathways were significantly enriched (Table S2). In the US-270 vs. CK comparison, 145 pathways were annotated and 5 of them were significantly enriched. There were 3 pathways were significantly enriched with 321 DEPs in the US-360 vs. CK comparison. Notably, "ABC transporters" was the overlapping KEGG pathway encountered, and it was dominated by up-regulated DEPs.

3.4. Energy metabolism of Salmonella after exposure to HIU

In the annotation and enrichment analysis of DEPs, many DEPs were annotated as participating in energy metabolism. Oxidative phosphorylation is an essential part of bacterial energy metabolism. We found 26, 4, and 11 oxidative phosphorylation-related proteins significantly upregulated by US-270, US-90, and US-360 treatments, respectively. They mainly include ATP synthase subunit a (AtpB), ATP synthase subunit b (AtpF), NADH-quinone oxidoreductase subunit I (NuoI), FAD-dependent oxidoreductase (Ndh), succinate dehydrogenase flavoprotein subunit (SdhA), succinate dehydrogenase cytochrome *b*556 subunit (SdhC), cytochrome bo(3) ubiquinol oxidase subunit 1 (CyoB), and cytochrome bd-I ubiquinol oxidase subunit (CydA). All of these proteins are key enzymes that function in the oxidative respiration electron transport chain (Fig. 4A). For example, ATP synthase subunit a (AtpB) is one of the critical proteins forming the proton channel and it is pivotal for enabling the transmembrane transport of protons. NADH-quinone oxidoreductase subunit I (NuoI) plays an important role in the electron transport chain by participating in electron transfer and linking redox reactions to proton shifts (Erhardt et al., 2014). Therefore, the upregulation of these key proteins improves the cells' ability to cope with the enhanced energy metabolism and osmotic pressure changes induced by ultrasound exposure. Moreover, the US-270 treatment caused greater upregulation of oxidative phosphorylation-related proteins. This suggests *Salmonella* requires more intense regulation when treated by US-270 in order to withstand the impaired energy metabolism caused by HIU.

Unlike the upregulated oxidative phosphorylation induced by HIU, the TCA cycle of *Salmonella* was downregulated and blocked. We found that treating bacteria with US-270 caused their upregulation of six TCA cycle-related proteins and downregulation of four, while exposure to US-90 or US-360 caused the upregulation of only one protein in *Salmonella*.

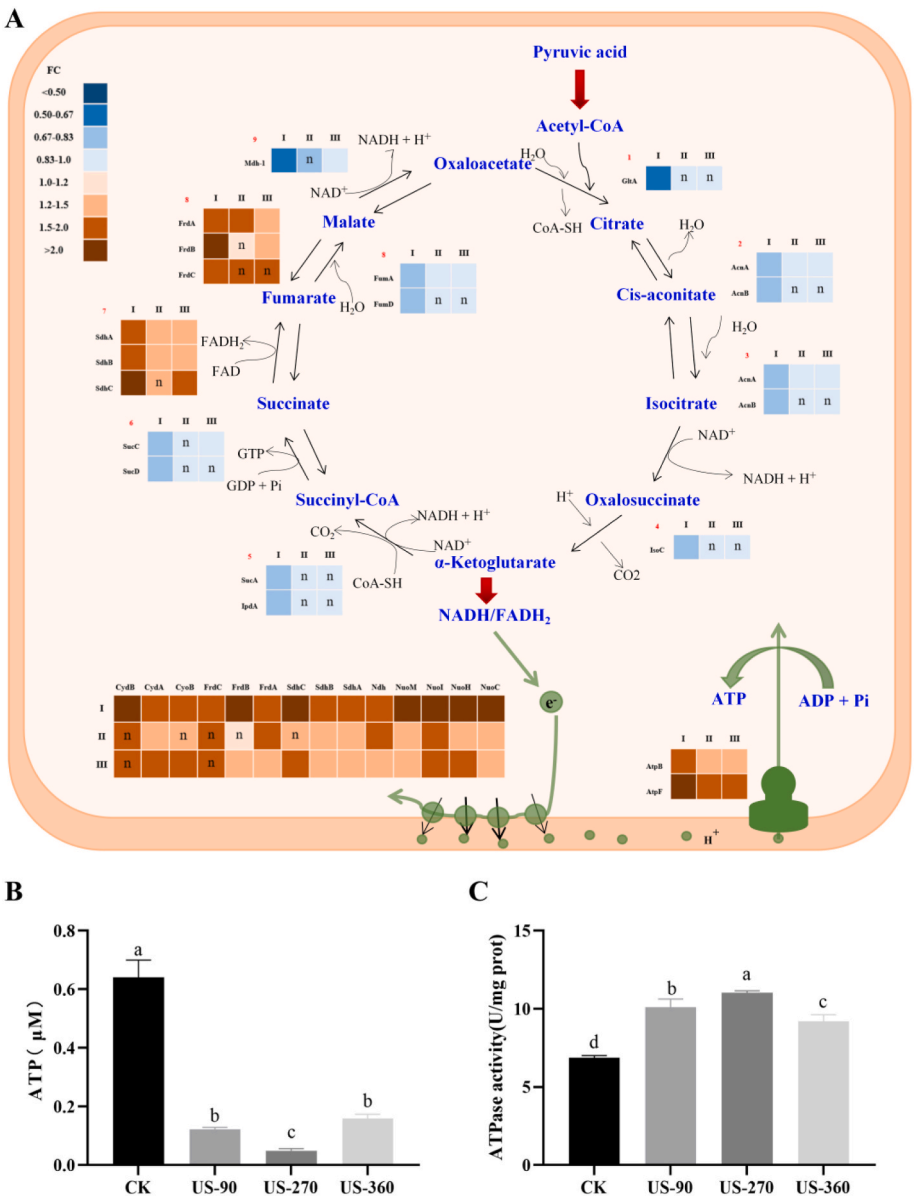

Fig. 4. Effects of high-intensity ultrasound (HIU) treatment on the energy metabolism of *Salmonella*. (A) Changes in the expression of proteins associated with oxidative phosphorylation and the TCA cycle. **(B)** Intracellular ATP content of *Salmonella*. **(C)** Intracellular ATPase activity of *Salmonella*. CK, untreated group; US-90, 90 W for 25 min; US-270, 270 W for 15 min; US-360, 360 W for 5 min. I, US-270/CK; II, US-90/CK; III, US-360/CK.

The upregulated proteins were mainly succinate dehydrogenase subunits (SdhA, SdhB, SdhC) and fumarate reductase subunits (FrdA, FrdB, FrdC). Interestingly, these upregulated TCA cycle-related DEPs were all involved in oxidative phosphorylation. Nonetheless, other related proteins involved in the TCA cycle were downregulated, to some extent, among which rate-limiting enzymes, namely citrate synthase (GltA) and malate dehydrogenase (Mdh_1), were significantly downregulated (Fig. 4A).

The energy metabolism pathways of *Salmonella* were evidently changed by the HIU treatment, which inevitably affected its energy production. Accordingly, we measured both the ATP content and ATPase activity of those *Salmonella* cells left by the HIU treatment. Compared with the untreated group (0.64 μM), the intracellular ATP content of *Salmonella* cells after their exposure to the US-90 and US-360 treatments had dropped sharply, to 0.12 and 0.16 μM, respectively; and even lower, to 0.05 μM, after the US-270 treatment (Fig. 4B). These results are consistent with other reports of the intracellular ATP content of bacteria decreasing significantly after ultrasound treatments (Li et al., 2018; Lin et al., 2019). *Salmonella*'s decreased ATP content might be due to much energy consumed in responding to HIU-induced physiological stress, as well as the possible ATP leakage due to the enhanced cell wall-membrane permeability. Importantly, ATPase activity in *Salmonella* cells increased from 6.86 U/mg protein to 9.18–11.02 U/mg protein after treating them with HIU, reached its maximum under the 270-US treatment (Fig. 4C). This augmented ATPase activity in HIU-treated *Salmonella* cells concurs with the upregulation of oxidative phosphorylation-related enzymes, implicating a stress response to HIU in bacterial cells.

The above findings strongly suggest that the lethal effect of HIU is closely linked to its inhibitory effect on *Salmonella*'s energy metabolism-related proteins. Similar findings were reported by other investigators. For example, Li et al. found upregulation of ATP synthase was not effective in reversing the decrease in ATP production of *E. coli O157:H7* cells under sonication (Li et al., 2021); further transcriptomic analysis confirmed that genes encoding TCA cycle-related enzymes were downregulated, which could lessen the accumulation of intracellular NADH

and $FADH_2$. Under the stress imposed by HIU, *Salmonella* cells respond by consuming a large amount of ATP and upregulating their oxidative phosphorylation, in an attempt to enhance their energy supply. Nevertheless, the key enzymes of the TCA cycle were downregulated, so that the upstream supply of energy is interrupted. Furthermore, an inability to effectively supply ATP would be extremely detrimental to the cellular repair of stress damage and regulation of substance uptake by *Salmonella* cells. Therefore, we surmise that if energy metabolism can be further blocked while undergoing the HIU treatment, the sterilization effect on *Salmonella* ought to be effectively enhanced.

3.5. Stress response of Salmonella to the HIU treatment

Bacteria have a complex regulatory network to resist and repair damage caused by stressful abiotic conditions (e.g., pH, cold/heat, UV radiation, oxidation, and osmotic pressure) (Sarjit et al., 2019). We found that, in response to the HIU treatment, *Salmonella* undergo different degrees of regulated expression of their signal transduction, chemotaxis, and material transport, so as to maximally adapt to HIU-induced stresses. The exertion of these regulatory effects is also likely a major reason why the HIU treatment was not effective at completely inhibiting the bacteria.

First, for the bacterial cells to perceive external stimuli, the response of the two-component system is inseparable (van Hoek et al., 2019). In the present study, in response to the US-270 treatment, 74 two-component system-related proteins were differentially expressed (65 upregulated, 9 downregulated), whereas treatment with US-90 elicited 21 such DEPs, consisting of 20 upregulated and 1 downregulated, and that with US-360 induced 22 DEPs, of which 19 were upregulated and 3 downregulated. Moreover, although the lethality to *Salmonella* under exposure to US-90 and US-360 was similar, the responsive regulation of the two-component system differed. There were 9 DEPs in the comparison between the US-90 and US-360 groups, this probably caused by the difference in the power setting of the HIU treatment. Compared with the US-90 and US-360 treatments, applying US-270 caused a broader and deeper range of protein upregulation. Notably, DEPs induced under US-90 and US-360 treatments were a subset of the US-270-induced DEPs. Among the two-component system-related DEPs induced by the three HIU treatments, 15 DEPs overlapped (Fig. 5A). Some of these DEPs are key proteins used by bacteria to sense changes in their external environment. For example, the Rcs signaling system, consisting of sensor histidine kinase (RcsC) and phosphotransferase (RcsD), could detect outer membrane defects in time and then regulate the transcription level of cupD accordingly, which in turn modulates the formation of biofilm and the appearance of fimbriae (Costa et al., 2003; Nicastro et al., 2009). Therefore, signal transduction is the key process determining microorganisms' response to one or more environmental stress factors. In this study, the extensive upregulation of *Salmonella*'s two-component system-related proteins presumably initiated a suite of regulation activity in response to HIU stress.

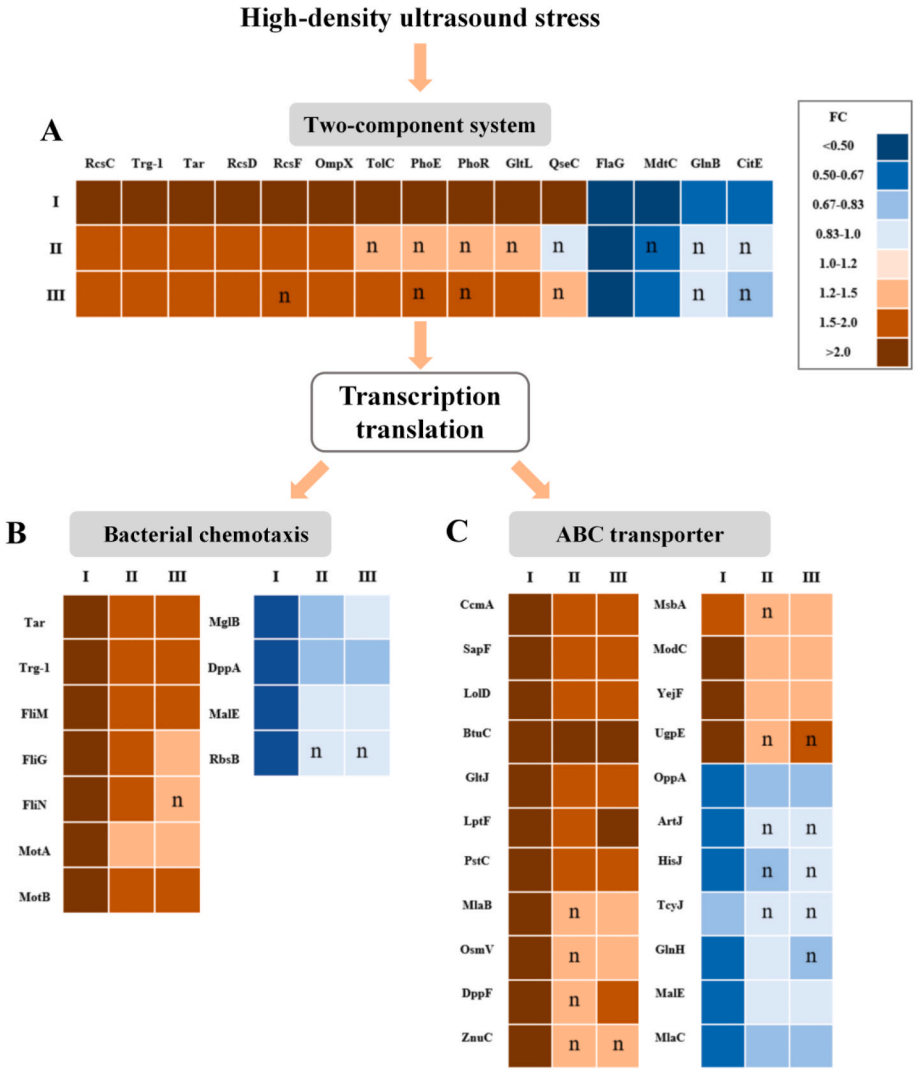

Fig. 5. Regulatory mechanisms of *Salmonella* in response to high-intensity ultrasound (HIU) treatment. (A) Changes in the expression of proteins associated with the two-component system. **(B)** Changes in the expression of proteins associated with bacterial chemotaxis. **(C)** Changes in the expression of proteins associated with the ABC transporter. CK, untreated group; US-90, 90 W for 25 min; US-270, 270 W for 15 min; US-360, 360 W for 5 min. Inside the box, "n" indicates $P > 0.05$. I, US-270/CK; II, US-90/CK; III, US-360/CK.

The two-component system activated by HIU might further regulate the chemotaxis and flagella assembly of *Salmonella*. Our results show that treatment with US-270 causes the differential expression of 16 bacterial chemotaxis-related proteins (12 upregulated, 4 downregulated), and similar changes were also found in US-90- and US-360-treated *Salmonella*. Seven upregulated DEPs overlapped among the chemotaxis-related DEPs induced by the three HIU treatments (Fig. 5B). Two of these flagellar motility switch proteins (FliN and FliM)—which constitute the rotor-mounted switch complex (C-loop) interacting with CheY and CheZ chemotaxis proteins—are known to figure prominently in bacterial flagellar motility (Delalez et al., 2010). Therefore, upregulation of these DEPs related to chemotaxis and flagella assembly suggests that the chemotactic movement of *Salmonella* was enhanced by the HIU treatment. *Salmonella* tried to avoid the stress incurred from exposure to HIU, by gaining better access to material components required for a stress response, that is via enhanced chemotaxis to move towards a favorable (i.e., less stressful) environment. If so, we surmise that inhibiting the chemotaxis of *Salmonella* should further enhance the bactericidal effect of HIU.

While enhancing their chemotaxis, *Salmonella* cells also upregulated the transport of substances within them in response to HIU-induced stress. The ATP binding cassette (ABC) transporter is responsible for the transmembrane transport of nutrients, and is essential for the uptake of substances by *Salmonella* (Rismondo and Schulz, 2021). Here, we distinguished 92 ABC transporter-related proteins that were differentially expressed after treating *Salmonella* with US-270 (72 upregulated, 20 downregulated); the US-360 treatment caused the upregulation of 33 ABC transporter-related DEPs; and applying the US-90 treatment upregulated 19 ABC transporter-related DEPs but downregulated just 1 DEP. Overall, we found 15 commonly upregulated ABC-related proteins in *Salmonella* in response to the HIU treatment (Fig. 5C). Such as vitamin B_{12} import system permease protein (BtuC), peptide transporter ATP-binding protein (SapF), amino acid ABC transporter permease (GltJ), phosphate transport system permease protein (PstC). This massive upregulation of ABC transporter proteins would accelerate the transport of vitamin B12, peptides, amino acids, and phosphates (Davies et al., 2021). Yet some of ABC transporter-related DEPs were downregulated by the HIU treatment; Such as oligopeptide ABC transporter substrate binding protein (OppA), glutamine ABC transporter substrate binding protein (GlnH), and maltodextrin binding protein (MalE) were all downregulated. The decrease in these transporter proteins may be due to ultrasound treatment interfering with the transcriptional-translational process of these proteins, which leads to a decrease in content and thus affects the uptake of these substances by the cells. In a study, ultrasound has been found to inhibit the expression of ABC transporter protein genes associated with *E. coli* (Li et al., 2021). It was also possible that the cells were actively regulated in order to reduce unnecessary energy consumption, but further studies were needed. Thus, combining the application of HIU with an inhibitor capable of blocking ABC transport is expected to be effective at reducing the survival probability of *Salmonella*.

These results of quantitative proteomics provide valuable information for further strengthening the bactericidal ability of HIU against *Salmonella*. HIU downregulates the TCA cycle of *Salmonella* and blocks the production of ATP. The fatal energy shortage might render many HIU-treated *Salmonella* unculturable. Therefore, making full use of the blocking effect of HIU upon ATP production to enhance the lethality of HIU against *Salmonella* is a promising strategy that deserves special attention in future studies. However, to cope with the stress from HIU, *Salmonella* activated the two-component system to regulate their chemotaxis and substance uptake. These stress regulation activities might explain why a small number of *Salmonella* could still be culturable after incurring an HIU treatment. Among these regulatory pathways of *Salmonella* forming its response to HIU, the two-component system is consider more critical because this pathway enables the transduction of pressure signals and this shapes *Salmonella*'s response to HIU. Therefore, disrupting the two-component system of *Salmonella* ought to interfere or cripple its efforts to cope with HIU-induced stress, which would greatly improve the sterilization ability of HIU.

4. Conclusion

The results showed that treating *Salmonella* with HIU resulted in the disintegration of its structure and leakage of intracellular substances, which significantly reduced the number of cultured *Salmonella*. Some incompletely disintegrated *Salmonella* try to survive via enhanced environmental sensing, chemotaxis, substance uptake, and ATP production. However, the structural damage and blocked expression of some key proteins generally impairs the performance of these regulated stress repair functions. These findings contribute to a better understanding of the survival mechanisms of *Salmonella* under various HIU treatments. On this basis, applying measures targeting the above-mentioned regulatory pathways (TCA cycle, oxidative phosphorylation, two-component system, ABC transport, and bacterial chemotaxis) in combination with HIU will hopefully achieve a more effective inactivation of *Salmonella* in food products.

Funding

This work was supported by the National Natural Science Foundation of China (grant numbers 32072236, 31970092).

CRediT authorship contribution statement

Wei Luo: Investigation, Data curation, Formal analysis, Writing – original draft. **Jinqiu Wang:** Methodology, Resources, Writing – review & editing, Project administration. **Yan Chen:** Investigation. **Yixu Wang:** Investigation. **Rui Li:** Methodology, Resources. **Jie Tang:** Writing – review & editing. **Fang Geng:** Conceptualization, Writing – original draft, Writing – review & editing, Supervision, Funding acquisition.

Declaration of competing interest

The authors declare that they have no known competing financial interests or personal relationships that could have appeared to influence the work reported in this paper.

Appendix A. Supplementary data

Supplementary data to this article can be found online at https://doi.org/10.1016/j.crfs.2022.09.029.

References

Ashburner, M., Ball, C.A., Blake, J.A., Botstein, D., Cherry, J.M., 2000. Gene ontology: tool for the unification of biology. The Gene Ontology Consortium. Nat. Genet. 25 (1), 25–29. https://doi.org/10.1038/75556.

Bi, X., Wang, X., Chen, Y., Chen, L., Xing, Y., Che, Z., 2020. Effects of combination treatments of lysozyme and high power ultrasound on the Salmonella typhimurium inactivation and quality of liquid whole egg. Ultrason. Sonochem. 60, 104763 https://doi.org/10.1016/j.ultsonch.2019.104763.

Cacciatore, F.A., Brandelli, A., Malheiros, P., 2020. Combining natural antimicrobials and nanotechnology for disinfecting food surfaces and control microbial biofilm formation. Crit. Rev. Food Sci. Nutr. (1), 1–12. https://doi.org/10.1080/10408398.2020.1806782.

Chen, F., Zhang, M., Yang, C., 2020. Application of ultrasound technology in processing of ready-to-eat fresh food: a review. Ultrason. Sonochem. 63, 104953 https://doi.org/10.1016/j.ultsonch.2019.104953.

Costa, C.S., Pettinari, M.J., Méndez, B.S., Antón, D.N., 2003. Null mutations in the essential gene yrfF (mucM) are not lethal in rcsB, yojN or rcsC strains of Salmonella enterica serovar Typhimurium. FEMS (Fed. Eur. Microbiol. Soc.) Microbiol. Lett. 222 (1), 25–32. https://doi.org/10.1016/S0378-1097(03)00221-0.

Dai, J., Bai, M., Li, C., Cui, H., Lin, L., 2020. Advances in the mechanism of different antibacterial strategies based on ultrasound technique for controlling bacterial contamination in food industry. Trends Food Sci. Technol. 105, 211–222. https://doi.org/10.1016/j.tifs.2020.09.016.

Davies, J., Currie, M., Wright, J., Newton-Vesty, M., North, R., Mace, P., Allison, J., Dobson, R., 2021. Selective nutrient transport in bacteria: multicomponent transporter systems reign supreme. Front. Mol. Biosci. 8, 699222 https://doi.org/10.3389/fmolb.2021.699222.

Delalez, N.J., Wadhams, G.H., Rosser, G., Xue, Q., Brown, M.T., Dobbie, I.M., Berry, R. M., Leake, M.C., Armitage, J.P., 2010. Signal-dependent turnover of the bacterial flagellar switch protein FliM. Proc. Natl. Acad. Sci. USA 107 (25), 11347. https://doi.org/10.1073/pnas.1000284107.

Duarte, A.L.A., do Rosário, D.K.A., Oliveira, S.B.S., de Souza, H.L.S., de Carvalho, R.V., Carneiro, J.C.S., Silva, P.I., Bernardes, P.C., 2018. Ultrasound improves antimicrobial effect of sodium dichloroisocyanurate to reduce Salmonella Typhimurium on purple cabbage. Int. J. Food Microbiol. 269, 12–18. https://doi.org/10.1016/j.ijfoodmicro.2018.01.007.

Erhardt, H., Dempwolff, F., Pfreundschuh, M., Riehle, M., Schäfer, C., Pohl, T., Graumann, P., Friedrich, T., 2014. Organization of the Escherichia coli aerobic enzyme complexes of oxidative phosphorylation in dynamic domains within the cytoplasmic membrane. MICROBIOLOGYOPEN 3 (3), 316–326. https://doi.org/10.1002/mbo3.163.

European Food Safety, A., European Centre for Disease, P., Control, 2021. The European union one health 2020 zoonoses report. EFSA J. 19 (12), e06971 https://doi.org/10.2903/j.efsa.2021.6971.

Geng, F., Wen, X., Xu, Y., Zhang, M., Zhou, L., Liu, D., Li, X., Wang, J., 2021b. Phosphoinositide signaling plays a key role in the regulation of cell wall reconstruction during the postharvest morphological development of Dictyophora indusiata. Food Chem. 346, 128890 https://doi.org/10.1016/j.foodchem.2020.128890.

Geng, F., Xie, Y., Wang, J., Majumder, K., Qiu, N., Ma, M., 2018. N-glycoproteomic analysis of chicken egg yolk. J. Agric. Food Chem. 66 (43), 11510–11516. https://doi.org/10.1021/acs.jafc.8b04492.

Geng, F., Xie, Y., Wang, Y., Wang, J., 2021a. Depolymerization of chicken egg yolk granules induced by high-intensity ultrasound. Food Chem. 354, 129580 https://doi.org/10.1016/j.foodchem.2021.129580.

He, Q., Guo, M., Jin, T.Z., Arabi, S.A., Liu, D., 2021. Ultrasound improves the decontamination effect of thyme essential oil nanoemulsions against Escherichia coli O157: H7 on cherry tomatoes. Int. J. Food Microbiol. 337, 108936 https://doi.org/10.1016/j.ijfoodmicro.2020.108936.

Hu, Y., Nie, W., Hu, X., Li, Z., 2016. Microbial decontamination of wheat grain with superheated steam. Food Control 62, 264–269. https://doi.org/10.1016/j.foodcont.2015.11.001.

José, J.F. B.d.S., Ramos, A.M., Vanetti, M.C.D., Andrade, N.J.d., 2021. Inactivation of Salmonella Enteritidis on Cherry Tomatoes by Ultrasound, Lactic Acid, Detergent, and Silver Nanoparticles, vol. 67, pp. 259–270. https://doi.org/10.1139/cjm-2020-0013, 3.

Kaavya, R., Pandiselvam, R., Abdullah, S., Sruthi, N.U., Jayanath, Y., Ashokkumar, C., Chandra Khanashyam, A., Kothakota, A., Ramesh, S.V., 2021. Emerging non-thermal technologies for decontamination of Salmonella in food. Trends Food Sci. Technol. 112, 400–418. https://doi.org/10.1016/j.tifs.2021.04.011.

Laranja, D.C., da Silva Malheiros, P., Cacciatore, F.A., de Oliveira Elias, S., Milnitsky, B. P., Tondo, E.C., 2021. Salmonella inactivation and changes on texture and color of chicken skin treated with antimicrobials and ultrasound. Lebensm. Wiss. Technol. 149, 111836 https://doi.org/10.1016/j.lwt.2021.111836.

Li, J., Ding, T., Liao, X., Chen, S., Ye, X., Liu, D., 2017. Synergetic effects of ultrasound and slightly acidic electrolyzed water against Staphylococcus aureus evaluated by flow cytometry and electron microscopy. Ultrason. Sonochem. 38, 711–719. https://doi.org/10.1016/j.ultsonch.2016.08.029.

Li, J., Liu, D., Ding, T., 2021. Transcriptomic analysis reveal differential gene expressions of Escherichia coli O157:H7 under ultrasonic stress. Ultrason. Sonochem. 71, 105418 https://doi.org/10.1016/j.ultsonch.2020.105418.

Li, J., Ma, L., Liao, X., Liu, D., Lu, X., Chen, S., Ye, X., Ding, T., 2018. Ultrasound-induced Escherichia coli O157:H7 cell death exhibits physical disruption and biochemical apoptosis. Front. Microbiol. 9, 2486. https://doi.org/10.3389/fmicb.2018.02486.

Li, J., Zhang, X., Ashokkumar, M., Liu, D., Ding, T., 2020. Molecular regulatory mechanisms of Escherichia coli O157:H7 in response to ultrasonic stress revealed by proteomic analysis. Ultrason. Sonochem. 61, 104835 https://doi.org/10.1016/j.ultsonch.2019.104835.

Li, W., Pires, S.M., Liu, Z., Ma, X., Liang, J., Jiang, Y., Chen, J., Liang, J., Wang, S., Wang, L., Wang, Y., Meng, C., Huo, X., Lan, Z., Lai, S., Liu, C., Han, H., Liu, J., Fu, P., Guo, Y., 2020. Surveillance of foodborne disease outbreaks in China, 2003–2017. Food Control 118, 107359. https://doi.org/10.1016/j.foodcont.2020.107359.

Lin, L., Wang, X., Li, C., Cui, H., 2019. Inactivation mechanism of E. coli O157:H7 under ultrasonic sterilization. Ultrason. Sonochem. 59, 104751 https://doi.org/10.1016/j.ultsonch.2019.104751.

Liu, H., Li, Z., Zhang, X., Liu, Y., Hu, J., Yang, C., Zhao, X., 2021a. The effects of ultrasound on the growth, nutritional quality and microbiological quality of sprouts. Trends Food Sci. Technol. 111, 292–300. https://doi.org/10.1016/j.tifs.2021.02.065.

Liu, X., Wang, J., Liu, L., Cheng, L., Huang, Q., Wu, D., Peng, L., Shi, X., Li, S., Geng, F., 2021b. Quantitative N-glycoproteomic analyses provide insights into the effects of thermal processes on egg white functional properties. Food Chem. 342, 128252 https://doi.org/10.1016/j.foodchem.2020.128252.

Liu, X., Wang, J., Huang, Q., Cheng, L., Gan, R., Liu, L., Wu, D., Li, H., Peng, L., Geng, F., 2020. Underlying mechanism for the differences in heat-induced gel properties between thick egg whites and thin egg whites: gel properties, structure and quantitative proteome analysis. Food Hydrocolloids 106, 105873. https://doi.org/10.1016/j.foodhyd.2020.105873.

Luo, W., Wang, J., Wang, Y., Tang, J., Ren, Y., Geng, F., 2021. Bacteriostatic effects of high-intensity ultrasonic treatment on Bacillus subtilis vegetative cells. Ultrason. Sonochem. 81, 105862 https://doi.org/10.1016/j.ultsonch.2021.105862.

Nicastro, G.G., Boechat, A.L., Abe, C.M., Kaihami, G.H., Baldini, R.L., 2009. Pseudomonas aeruginosa PA14 cupD transcription is activated by the RcsB response regulator, but repressed by its putative cognate sensor RcsC. FEMS (Fed. Eur. Microbiol. Soc.) Microbiol. Lett. 301 (1), 115–123. https://doi.org/10.1111/j.1574-6968.2009.01803.x.

Pereira Batista, A.F., Rodrigues dos Santos, A., Fiori da Silva, A., Coelho Trevisan, D.A., Ribeiro, L.H., Zanetti Campanerut-Sá, P.A., Alves de Abreu Filho, B., Junior, M.M., Graton Mikcha, J.M., 2019. Inhibition of Salmonella enterica serovar Typhimurium by combined carvacrol and potassium sorbate in vitro and in tomato paste. Lebensm. Wiss. Technol. 100, 92–98. https://doi.org/10.1016/j.lwt.2018.10.006.

Qi, Y., Zhao, W., Wang, T., Pei, F., Yue, M., Li, F., Liu, X., Wang, X., Li, H., 2020. Proteomic analysis of the antimicrobial effects of sublethal concentrations of thymol on Salmonella enterica serovar Typhimurium. Appl. Microbiol. Biotechnol. 104 (8), 3493–3505. https://doi.org/10.1007/s00253-020-10390-9.

Rismondo, J., Schulz, L.M., 2021. Not just transporters: alternative functions of ABC transporters in Bacillus subtilis and Listeria monocytogenes. Microorganisms 9 (1), 163. https://doi.org/10.3390/microorganisms9010163.

Ross, P, L., 2004. Multiplexed protein quantitation in Saccharomyces cerevisiae using amine-reactive isobaric tagging reagents. Mol. Cell. Proteomics 3 (12), 1154–1169. https://doi.org/10.1074/mcp.M400129-MCP200.

Sarjit, A., Ravensdale, J.T., Coorey, R., Fegan, N., Dykes, G.A., 2019. Salmonella response to physical interventions employed in red meat processing facilities. Food Control 103, 91–102. https://doi.org/10.1016/j.foodcont.2019.03.038.

Seo, M.K., Jeong, H.L., Han, S.H., Kang, I., Ha, S.D., 2019. Impact of ethanol and ultrasound treatment on mesophilic aerobic bacteria, coliforms, and Salmonella Typhimurium on chicken skin. Poultry Sci. 98 (12), 6954–6963. https://doi.org/10.3382/ps/pez486.

Suginta, W., Sritho, N., Ranok, A., Bulmer, D.M., Kitaoku, Y., van den Berg, B., Fukamizo, T., 2018. Structure and function of a novel periplasmic chitooligosaccharide-binding protein from marine Vibrio bacteria. J. Biol. Chem. 293 (14), 5150–5159. https://doi.org/10.1074/jbc.RA117.001012.

Tao, Y., Qian, L.H., Xie, J., 2011. Effect of chitosan on membrane permeability and cell morphology of Pseudomonas aeruginosa and Staphyloccocus aureus. Carbohydr. Polym. 86 (2), 969–974. https://doi.org/10.1016/j.carbpol.2011.05.054.

van Hoek, M.L., Hoang, K.V., Gunn, J.S., 2019. Two-component systems in francisella species. Front. Cell. Infect. Microbiol. 9 https://doi.org/10.3389/fcimb.2019.00198, 198-198.

Wang, J., Liu, X., Li, S., Ye, H., Luo, W., Huang, Q., Geng, F., 2022b. Ovomucin may be the key protein involved in the early formation of egg-white thermal gel. Food Chem. 366, 130596 https://doi.org/10.1016/j.foodchem.2021.130596.

Wang, J., Xiao, J., Liu, X., Gao, Y., Luo, Z., Gu, X., Zhang, J., Wu, D., Geng, F., 2021. Tandem mass tag-labeled quantitative proteomic analysis of tenderloins between Tibetan and Yorkshire pigs. Meat Sci. 172, 108343 https://doi.org/10.1016/j.meatsci.2020.108343.

Wang, Y., Wang, J., Shi, Y., Ye, H., Luo, W., Geng, F., 2022a. Quantitative proteomic analyses during formation of chicken egg yolk. Food Chem. 374, 131828 https://doi.org/10.1016/j.foodchem.2021.131828.

Xie, Y., Wang, J., Wang, Y., Wu, D., Liang, D., Ye, H., Cai, Z., Ma, M., Geng, F., 2020. Effects of high-intensity ultrasonic (HIU) treatment on the functional properties and assemblage structure of egg yolk. Ultrason. Sonochem. 60, 104767 https://doi.org/10.1016/j.ultsonch.2019.104767.

Zhang, J., Wang, D., Sun, J., Sun, Z., Liu, F., Du, L., Wang, D., 2021. Synergistic antibiofilm effects of ultrasound and phenyllactic acid against Staphylococcus aureus and Salmonella enteritidis. Foods 10 (9), 2171. https://doi.org/10.3390/foods10092171.